

This is the accepted manuscript made available via CHORUS. The article has been published as:

Suppression of $\mu^{\{+\}}$ depolarization by fast magnetic fluctuations at avoided level crossings for $\text{Ho}^{\{3+\}}$ ions in CaWO_4

E. Kenney, A. Amato, S. R. Giblin, B. Z. Malkin, and M. J. Graf

Phys. Rev. B **98**, 134424 — Published 15 October 2018

DOI: [10.1103/PhysRevB.98.134424](https://doi.org/10.1103/PhysRevB.98.134424)

Suppression of μ^+ depolarization by fast magnetic fluctuations at avoided level crossings for Ho^{3+} ions in CaWO_4

E. Kenney¹, A. Amato², S. R. Giblin³, B. Z. Malkin⁴, and M. J. Graf¹

¹ Department of Physics, Boston College, Chestnut Hill, MA 02467 USA

² Paul Scherrer Institute, CH 5232 Villigen PSI, Switzerland

³ School of Physics and Astronomy, Cardiff University, Cardiff CF24 3AA, UK

⁴ Kazan Federal University, Kremlevskaya 18, Kazan 420008, Russian Federation

ABSTRACT

We use transverse field muon spin rotation to probe the low field dynamics of Ho^{3+} ions imbedded in a single crystal host matrix of CaWO_4 . The Ho^{3+} ions at sites with the full tetragonal symmetry of the crystal have avoided level crossings of hyperfine sublevels of the ground crystal-field doublet, resulting in measurable changes in the both the AC susceptibility and transverse field muon depolarization rate. The host material has primarily non-magnetic nuclear species and no magnetic ions, and so the muon is shown to be a direct non-resonant probe of pronounced changes of relaxation rates of the coupled electron-nuclear excitations of Ho^{3+} at avoided level crossings.

I. INTRODUCTION

The properties of nearly isolated spins in a solid host are of fundamental interest, exhibiting quantum dynamical phenomena, *e.g.* tunneling of magnetization [1], and which offer future application potential such as memory storage and quantum computing. The spin dynamics of Ho^{3+} ions lightly doped into the tetragonal single crystal host material LiYF_4 ('LYF:Ho') proved to be a useful paradigm system: the high quality and well-characterized host matrix provided a system whereby theoretical modeling based on known physical parameters could be used to describe the spin dynamics observed through magnetization [2], AC susceptibility [3 – 5] and nuclear magnetic resonance [6, 7]. The holmium ions substitute for yttrium trivalent ions at sites with S_4 point symmetry. The lowest multiplet $^5\text{I}_8$ of Ho^{3+} ions in the crystal field of tetragonal LiYF_4 is split into singlets Γ_1 and Γ_2 and non-Kramers doublets Γ_{34} (Γ are the

corresponding irreducible representations of the S_4 group). The ground state is a magnetic doublet (g -factor ≈ 13 for fields along the c -axis, and zero in the a - b plane) separated from the first excited singlet Γ_2 by approximately 10 K [2]. Due to the strong hyperfine coupling, the $I = 7/2$ Ho nucleus further splits this doublet into 8 doubly degenerate levels, separated from one another in zero field by approximately 0.22 K. Application of a weak magnetic field $\mathbf{B} \parallel \mathbf{c}$ lifts this degeneracy and results in a sequence of level crossings at fields of $B_n = 23n$ mT, where n is an integer and $-7 \leq n \leq 7$ [2]. The low temperature, low magnetic field spin dynamics are dominated by the presence of fairly large avoided level crossings (ALCs) when n is odd [2, 8], corresponding to transitions between the hyperfine sublevels where the change in the nuclear spin projections on the symmetry axis ($z \parallel c$) $\Delta I_z = 2$; these large tunneling gaps result from mixing of wave functions of the ground state doublet and the first excited singlet by the hyperfine interaction. Smaller random strain-induced gaps are also present at $\Delta I_z = 0$ crossings at field values corresponding to odd values of n (see Inset in Fig. 1) [9].

Transverse field muon spin rotation (μ SR) experiments on LYF:Ho [8] provided an unusual mechanism for probing the change in spin dynamics at these ALCs. Sharp dips were observed in the muon transverse field depolarization rate λ_{TF} at field values corresponding to $n = 1$ and 3, while a much smaller reduction was observed at $n = 2$. It was proposed that the depolarization was due to the nearly static disorder of the Ho^{3+} ions; however, near large gaps at ALCs the magnetic fluctuation rate increased significantly, thereby reducing the static disorder on the muon timescale and causing a decrease in λ_{TF} . Given the dilute Ho^{3+} ion distribution one outstanding concern is the nature of the muon coupling to the Ho^{3+} ions. It is known that the ^{19}F spin bath strongly couples to the Ho^{3+} ions [7], and the electronegative F^- ion strongly interacts with (indeed, *bonds to*) the implanted muons in a μ SR experiment [8, 10]. The presence of possible multiple muon depolarization channels calls into question the interpretation of the results from Ref. 8, and in particular whether or not the muon is directly probing the magnetic fluctuations of the Ho^{3+} ions. As described below, we can experimentally answer this question by removing the $\mu^+ - \text{F}^-$ depolarization channel. Thus, we have a quantifiable method of demonstrating the direct depolarization of the muon by dilute magnetic moments.

In this work we use transverse field μ SR to probe the low field dynamics of Ho^{3+} ions imbedded in a single crystal host matrix of Scheelite CaWO_4 ('CWO:Ho'). This host is

isostructural with LiYF_4 , and detailed studies via optical and EPR spectroscopy of $\text{CWO}:\text{Ho}$ showed that the energy level diagrams of Ho^{3+} in both hosts are qualitatively identical [11], although the heterovalent substitution required to maintain charge balance in $\text{CWO}:\text{Ho}$ (see below) creates a substantial number of Ho^{3+} centers lacking the tetragonal crystal symmetry. There is no electronic contribution to the magnetic properties from the valence electrons of the host matrix, and only very low concentrations of weak nuclear moments associated with the 14% ^{183}W and substitutional $^7\text{Li}^+$ impurities (see below), and so in this system there is no intermediary nuclear spin bath. We find very similar results to those presented in Ref. 8, demonstrating that the muon is indeed a direct probe of the Ho^{3+} spin dynamics, even when there are multiple possible relaxation channels present as in the case of $\text{LYF}:\text{Ho}$.

II. EXPERIMENTAL DETAILS AND RESULTS

The $\text{CWO}:\text{Ho}$ sample used in this work, with a nominal Ho concentration of 0.5%, was studied in Ref. 11, and was grown by Czochralski technique from Ho_2O_3 , WO_3 , CaCO_3 , and Li_2CO_3 . The Ho^{3+} substitutes for Ca^{2+} , and charge balance is maintained by Li^+ replacement of Ca^{2+} during growth.

AC susceptibility and DC magnetization measurements were made in a Quantum Design MPMS3 SQUID system. The DC magnetization at 2 K in fields up to 6 T (Fig. 1) showed that the actual Ho concentration in our sample was approximately 0.2%, as described below. The discrepancy with the nominal value is presumably due to the imperfect efficiency of Li^+ charge compensation. The magnetization and AC susceptibility data and the fits shown in Figs. 1 and 2 will be discussed later in this work.

In time-differential μSR , a spin-polarized μ^+ enters a sample, and within 10 ps or less it comes to rest, typically at one or two electrostatically favorable crystalline sites. In this work the specific stopping site is not relevant, given that the muon is interacting with dilute magnetic impurities. At some later time t the muon decays, and the resulting positron is preferentially emitted along the direction of the muon spin moment and detected. After several million decay events one creates a time histogram of the detector signal asymmetry $A(t)$ [12], which is proportional to the muon polarization and characterizes its response to the local magnetic fields at the muon stopping sites. We assume that the stopping sites as well as the impurity Ho^{3+} ions are distributed randomly in the sample volume. In transverse field mode, the initial muon

polarization has a component perpendicular to the applied magnetic field \mathbf{B} , resulting in muon precession. Variations of the local magnetic field between muon stopping sites produce a dephasing of $A(t)$ due to the spread of Larmor frequencies for the individual muon decay events, and so transverse field measurements are extremely sensitive to magnetic inhomogeneity.

The μ SR measurements were conducted on the General Purpose Spectrometer on the πM_3 continuous beamline at the Paul Scherrer Institute. The beam momentum and external magnetic field were aligned parallel to the crystalline c -axis. Experiments were conducted in a gas flow cryostat and our measurements span the range $1.6 \text{ K} \leq T \leq 20 \text{ K}$. We utilized the spin-rotated mode, where the muon spin is tilted approximately 50 degrees with respect to the beam momentum. The transverse field depolarization is then monitored with detectors oriented along a line perpendicular to the applied magnetic field.

In Fig. 2 we show the magnetic field variation of the AC susceptibility at a frequency of 953 Hz and AC amplitude of 1.5 Oe at 2 K; the oscillating magnetic field, as well as the constant field \mathbf{B} , was oriented along the c -axis. The out-of-phase component χ'' shows dips at the B_n values listed above [4, 5], while the in-phase component χ' has barely discernible peaks at B_n . We find the minima in χ'' exhibit an average spacing of roughly 22.9 mT; a comparison with the value of $B_1=23.1 \text{ mT}$ obtained from calculations (see Inset in Fig. 1) indicates a misalignment less than 3° of the applied field with the c -axis.

Zero-field muon-spin depolarization versus time data (not shown) were taken at 20 K. A very fast depolarization constituting 25% of the signal was observed, while the remaining signal was essentially constant in time. The fast relaxation originates from the formation of a bound pair μ^+e^- (muonium), see also below. We fit the slowly relaxing signal to a simple exponential decay, and find a depolarization rate of $0.04(1) \mu\text{s}^{-1}$, confirming the very small contribution of the host matrix to the observed relaxation. In Figure 3a we show the time dependent asymmetry of the muon at $T = 1.8 \text{ K}$ and in a magnetic field $\mathbf{B} \parallel c$ with $B = 20 \text{ mT}$. The signal consists of three components: two high frequency oscillatory signals evident at short times, along with a slow oscillation at the expected precession frequency $f_\mu = 2.71 \text{ MHz}$ which is determined by $f_\mu = (\gamma_\mu / 2\pi)B$, where γ_μ is the muon gyromagnetic ratio and $\gamma_\mu / 2\pi = 135.5 \text{ MHz/T}$. The short time signal was found to be independent of temperature below 20 K, so to accurately characterize it we summed all our data between 1.8 and 20 K, and this sum at short times is

shown in Fig. 3b. The fast oscillations have frequencies of 28.1(2) and 39.6(3) MHz at 20 mT, consistent with muonium formation as reported, for example, for silicon in Ref. 13. These correspond to the transitions between the muonium triplet states, for which the degeneracy is lifted by the applied magnetic field. So, our overall depolarization function (asymmetry normalized by its value at $t = 0$) was therefore fit to a three-component function

$$P(t) = \sum_{i=1}^3 a_i \exp[-(\lambda_i t)^{\beta_i}] \cos(2\pi f_i t + \phi_i) \quad (1)$$

where the first two terms ($i = 1, 2$) are associated with the muonium oscillations, and the third term with the precessing ‘free’ muon located at an interstitial site in the sample. These fits are shown as solid lines in Figs. 3a and 3b. We found that the a_i were constant, with $a_1 = 0.11(1)$, $a_2 = 0.15(1)$, and $a_3 = 0.74(3)$. Assuming constant values $\beta_1 = \beta_2 = 1$, we extracted fit values $\lambda_1 = 13(2) \mu\text{s}^{-1}$ and $\lambda_2 = 19(3) \mu\text{s}^{-1}$ which were assumed independent of temperature and field. The frequencies $f_{1,2}$ varied weakly with field (see Fig. 6) as expected for muonium in a low magnetic field. The phases were found to be $\phi_1 = -31(5)^\circ$, $\phi_2 = -10(5)^\circ$, and $\phi_3 = 5.3(1)^\circ$, and fixed at these values. The muon precession damping coefficient $\lambda_3 = \lambda_{TF}$ and exponent β_3 varied with both field and temperature.

The temperature dependence of λ_{TF} is shown in Fig. 4, along with β_3 in the inset. Because the crystal host is non-magnetic, damping is caused primarily by the Ho^{3+} ions. Near 20 K, the damping is quite weak and the exponent β_3 is roughly 1/3, which we interpret as the motional narrowing limit for thermally induced fluctuations of the Ho^{3+} moments [12]. As the temperature is lowered well below 13 K, only the lowest lying energy manifold is occupied and the rate of fluctuations is reduced substantially, with the exponent approaching a value of approximately $\beta_3 \approx 0.7$. This is smaller than the value ≈ 1.2 for Ho^{3+} ions in LYF [8] due to the lack of a contribution from quasistatic fluorine nuclear moments, which would have an expected exponent of 2 [8, 12]. This provides further evidence that the muon depolarization is modified solely by magnetism associated with Ho^{3+} , without complications from other sources of magnetism.

In Fig. 5 we show our results for the field dependence of λ_{TF} at low temperature ($T=1.6$ K), along with β_3 in the inset. Away from $n = 1$ (≈ 23 mT) the ‘background’ damping due to quasistatic magnetic inhomogeneity of dipolar fields produced by the Ho^{3+} ions is $0.5 \mu\text{s}^{-1}$, lower

than $0.9 \mu\text{s}^{-1}$ for LYF:Ho. Again, this is reasonably well accounted for by the absence of a contribution from the ^{19}F nuclei, which was determined to be $\approx 0.4 \mu\text{s}^{-1}$ from high temperature measurements [8]. A sharp dip, corresponding to a decrease of roughly 10% of λ_{TF} , is observed near 23 mT, along with a very weak structure near 46 mT, as observed in Ref. 8. The exponent β_3 is nearly field-independent. Finally, in Fig. 6 we show the weak magnetic field variation of f_1 and f_2 , which qualitatively agrees with field dependence observed for anomalous muonium in silicon [13].

III. DISCUSSION

The close similarity of the results obtained for LYF:Ho and CWO:Ho samples shows that the muon is responding directly to changes in rates of the Ho^{3+} dipolar magnetic fluctuations at the avoided level crossing $n = 1$, and neither the ^{19}F spin bath nor the possible broadening of the muon precession linewidth due to the formation of bound F- μ -F complexes [8] play a significant role in the observed decrease in the muon depolarization rate at the ALC. The muon is responding directly to the magnetic fluctuations of the Ho^{3+} ion. This confirms the general utility of transverse field μSR as non-resonant technique to probe spin dynamics at avoided level crossings.

To describe spectral and magnetic properties of Ho^{3+} ions, we considered the Hamiltonian

$$H = H_{FI} + H_{CF} + H_Z + H_{HFM} + H_{HFQ} \quad (2)$$

where H_{FI} is the standard parameterized free-ion Hamiltonian [14], H_{CF} is the crystal-field interaction, H_Z is the electronic Zeeman energy, H_{HFM} and H_{HFQ} are magnetic and electric quadrupole hyperfine interactions, respectively. Parameters of the free-ion Hamiltonian and crystal-field parameters for Ho^{3+} ions in CWO:Ho were presented in Ref. 11. All calculations mentioned in the present work involved numerical diagonalization of the Hamiltonian $H_0 = H_{FI} + H_{CF} + H_Z$ operating in the space of 1001 electronic states of the $4f^{10}$ configuration and subsequent diagonalization of the hyperfine interaction in the truncated basis of 520 electron-nuclear states corresponding to the electronic multiplets 5I_J ($J = 4 - 8$).

From Ref. 11, the important quantitative differences in the energy diagrams of Ho^{3+} at sites of tetragonal symmetry in CWO:Ho and LYF:Ho are: (a) the g -factor for $\mathbf{B} \parallel c$, g_{\parallel} , is slightly increased for CWO:Ho (13.7) compared to LYF:Ho (13.3); (b) the gap between the ground state doublet and first excited singlet is larger for CWO:Ho (13 K) than for LYF:Ho (10 K); (c) as a consequence of (b), the tunneling gaps Δ_1 at the avoided level crossings with $\Delta I_z = 2$ are reduced in CWO:Ho compared to LYF:Ho (according to calculations, $\Delta_1 = 220$ MHz in CWO:Ho and 305 MHz in LYF:Ho); and (d) the heterovalent doping required to maintain charge balance in CWO:Ho increases random strains in the crystal lattice relative to LYF:Ho. The increased strain in turn is expected to increase the size of a tunneling gap for an ALC with $\Delta I_z = 0$ [11], which is also present at the $n = 1$ field value. Taken in total, none of these will significantly alter the high frequency fluctuations at the ALCs, and this accounts for the close similarity between the transverse field μSR results for both systems. In contrast to the AC susceptibility data, the ALC near 46 mT ($n = 2$), which has very small tunneling gaps, is suppressed in both LYF:Ho and CWO:Ho when probed with μSR . Because the change in muon depolarization rate is sensitive to frequencies greater than the muon precession frequency (MHz range), it may be that μSR probes the adiabatic susceptibility as opposed to the isothermal susceptibility as measured by AC susceptibility in the kHz range. High frequency AC susceptibility measurements, in parallel with a theoretical investigation of the relevant relaxation mechanisms (*e.g.*, phonon and cross-relaxation processes [4, 5]) into the MHz range are underway to study this crossover further.

We now look more closely at the DC and AC magnetic measurements (Figs. 1 and 2). The changes in the AC susceptibility are far less dramatic than those reported for LYF:Ho. High-frequency EPR measurements on CWO:Ho [11] revealed the presence of Ho^{3+} ions in four distinct types of low-symmetry sites, in addition to the sites with tetragonal symmetry, which were attributed to the heterovalent doping. The Ho^{3+} ions in low symmetry environments have crystal field splittings and g -factors which are different than those of the ions at tetragonal sites. Moreover, the degeneracy of the electronic states is completely broken, and these Ho^{3+} ions at low temperature are in the singlet state and have only weak field-induced moments, so they exhibit none of the spin dynamics characteristic of the tetragonal site ions. To estimate the fraction of tetragonal sites, we have made a simple model to extend simulations as presented in

Refs. 5 and 10. We assume the Ho^{3+} ions are located at sites of either tetragonal [11] (subsystem A) or orthorhombic (subsystem B) symmetry. For simplicity, the rhombic crystal field component affecting ions in the subsystem B was defined by a single parameter $B_6^6 = 35 \text{ cm}^{-1}$, and the corresponding term $H_{\text{rh}} = B_6^6 O_6^6$ (O_6^6 is the Stevens operator) was added to the crystal field Hamiltonian used earlier in the analysis of the spectral and magnetic properties of the dominant tetragonal centers [11]. This term transforms the splitting of the ground doublet of tetragonal centers into two singlets with a gap of 6.8 K that is close to the average value of the gaps revealed by EPR measurements for low-symmetry centers. The two-site model was then used to fit the magnetization versus field data, as shown in Fig. 1; a diamagnetic contribution from the host crystal is also included. The estimated lower bound for Ho concentration is found to be 0.21%, with approximately equal fractions located at tetragonal and orthorhombic sites. We then fit the real and imaginary components of the AC susceptibility in an extension of the calculations carried out in Refs. 5 and 10. While this crude model adequately describes the qualitative results, it clearly under(over)-estimates magnitudes of the real(imaginary) components. A more complete model of the AC susceptibility, however, is well beyond the scope of this work. The relevant result for this work is that there is a concentration of approximately 0.1% of Ho^{3+} ions in a tetragonal environment, comparable to the 0.17% for the LYF:Ho samples studied in Ref. 8.

We can also estimate the tetragonal center concentration using the measured low-temperature depolarization rate λ_{TF} in a transverse magnetic field B of 20 mT, away from the $n = 1$ anticrossing. We assume that the muon interacts only with dilute magnetic impurities and that the resulting magnetic disorder is static on the muon timescale. Within this model we can calculate the λ_{TF} [15]. The magnetic moments of Ho^{3+} ions at sites with tetragonal symmetry are collinear to the c -axis and induce a local dipolar magnetic field with the components

$$B_{\text{dip},\alpha} = \pm(g_{\parallel}\mu_B / 2) \sum (3x_{\alpha}z - r^2\delta_{\alpha z}) / r^5 \quad (3)$$

at a muon placed at the center of the Cartesian system of coordinates $(z||c)$; in the low-field limit the Ho^{3+} in sites of orthorhombic symmetry are non-magnetic and do not contribute to the depolarization. Here the sum is taken over Ho^{3+} ions with the radius-vectors \mathbf{r} and coordinates x_{α} . The distribution function for the local dipolar field component B_{dip} along the external field considered in the framework of the continuum approximation can be written as follows [16]:

$$W(B_{dip}) = \frac{\Gamma}{\pi(B_{dip}^2 + \Gamma^2)} \quad (4)$$

where $\Gamma = 2\pi^2 g_{\parallel} \mu_B n_0 C / 9v$ is the distribution width in case of small concentration C of magnetic ions (here $n_0 = 2$ is the number of possible Ho positions in the unit cell with the volume $v = a^2 c / 2$, $a = 5.242 \text{ \AA}$ and $c = 11.372 \text{ \AA}$ are the CWO lattice constants [17]). By averaging a fixed muon contribution into the measured asymmetry $R \cos[\gamma_{\mu}(B + B_{dip})t]$ over the distribution (3), we obtain the time-dependent amplitude of the signal at the frequency f_{μ}

$$R(t) = R \int_{-\infty}^{\infty} \cos(\gamma_{\mu} B_{dip} t) W(B_{dip}) dB_{dip} = R \exp(-\gamma_{\mu} \Gamma t). \quad (5)$$

Note, we neglect here relaxation processes which bring stretched exponential time dependences [5]. Thus, the depolarization rate can be approximated by a rather simple expression

$$\lambda_{TF} = 8\pi^2 \gamma_{\mu} g_{\parallel} \mu_B C / 9a^2 c. \quad (6)$$

The measured λ_{TF} value of $0.5 \mu\text{s}^{-1}$ corresponds to the concentration $C=0.17 \%$ of the tetragonal centers that agrees satisfactorily with the analysis of the magnetization. The corresponding width Γ of the local field distribution equals 5.9 Oe .

IV. CONCLUSION

To summarize, we have studied the spin dynamics of Ho^{3+} ions imbedded in a single crystal host matrix of CaWO_4 . Three-quarters of the muons come to rest at interstitial crystal sites and probe the local magnetic field, while the remaining muons form muonium. Ions at sites with the full tetragonal symmetry of the crystal exhibit avoided level crossings, which produce fast fluctuations of local magnetic fields that suppress depolarization of muons precessing in the applied field. Our results confirm that this effect is not reliant on an intermediary spin bath, and so transverse field μSR is an effective non-resonant probe of magnetic fluctuations at avoided level crossings [8].

ACKNOWLEDGMENTS

Muon experiments were performed at the Swiss Muon Source at the Paul Scherrer Institute (Switzerland). Measurements in the MPMS3 system at Boston College were supported

in part by NSF grant DMR-1337567. BZM acknowledges the support by RFBR grant № 17-02-00403. We are grateful to Dr. Alexandra Tkachuk who provided the sample studied in this work.

* corresponding author (grafm@bc.edu)

References

- [1] L. Thomas, F. Lioni, R. Ballou, D. Gatteschi, R. Sessoli, and B. Barbara, *Nature (London)* **383**, 145 (1996); J. R. Friedman, M. P. Sarachik, J. Tejada, and R. Ziolo, *Phys. Rev. Lett.* **76**, 3830 (1996).
- [2] R. Giraud, W. Wernsdorfer, A.M. Tkachuk, D. Mailly, and B. Barbara, *Phys. Rev. Lett.* **87**, 057203 (2001).
- [3] R. Giraud, A. M. Tkachuk, and B. Barbara, *Phys. Rev. Lett.* **91**, 257204 (2003).
- [4] S. Bertaina, B. Barbara, R. Giraud, B. Z. Malkin, M. V. Vanuynin, A. I. Pominov, A. L. Stolov, and A. M. Tkachuk, *Phys. Rev. B* **74**, 184421 (2006).
- [5] R. C. Johnson, B. Z. Malkin, J. S. Lord, S. R. Giblin, A. Amato, C. Baines, A. Lascialfari, B. Barbara, and M. J. Graf, *Phys. Rev. B* **86**, 014427 (2012).
- [6] M. J. Graf, A. Lascialfari, F. Borsa, A. M. Tkachuk, and B. Barbara, *Phys. Rev. B* **73**, 024403 (2006).
- [7] B. Z. Malkin, M. V. Vanyunin, M. J. Graf, J. Lago, F. Borsa, A. Lascialfari, A. M. Tkachuk, and B. Barbara, *Eur. Phys. J. B* **66**, 155 (2008).
- [8] M. J. Graf, J. Lago, A. Lascialfari, A. Amato, C. Baines, S. R. Giblin, J. S. Lord, A. M. Tkachuk, and B. Barbara, *Phys. Rev. Lett.* **99**, 267203 (2007).
- [9] G. S. Shakurov, M. V. Vanyunin, B. Z. Malkin, B. Barbara, R. Yu. Abdulsabirov, S. L. Korableva, *Appl. Magn. Res.* **28**, 251 (2005).
- [10] R. C. Johnson, K. H. Chen, S. R. Giblin, J. S. Lord, A. Amato, C. Baines, B. Barbara, B. Z. Malkin, and M. J. Graf, *Phys. Rev. B* **83**, 174440 (2011).
- [11] G. S. Shakurov, E. P. Chukalina, M. N. Popova, B. Z. Malkin, and A. M. Tkachuk, *Phys. Chem. Chem. Phys.* **16**, 24727 (2014).
- [12] A. Yaouanc and P. Dalmas de Réotier, *Muon Spin Rotation, Relaxation, and Resonance: Applications to Condensed Matter* (Oxford University Press, New York, 2011).
- [13] R. F. Kiefl, M. Celio, T. L. Estle, S. R. Kreitzman, G. M. Luke, T. M. Riseman, and E. J. Ansaldo, *Phys. Rev. Lett.* **60**, 224 (1988).

- [14] W. T. Carnall, G. L. Goodman, K. Rajnak, and R. S. Rana, J. Chem. Phys. **90**, 3443 (1989).
- [15] See Ref. 12, section 6.6.2.
- [16] C. Held and M. W. Klein, Phys. Rev. Lett. **35**, 1783 (1975).
- [17] D. Errandonea and F. J. Manjón, Progress in Materials Science **53**, 711 (2008).

Figure Captions

FIG. 1. DC magnetization versus magnetic field directed along the tetragonal symmetry axis, along with the fit (solid line) as described in the text. Inset: Computed magnetic field dependences of the energies of the 16 lowest electron-nuclear states of Ho^{3+} ions in tetragonal centers. Points of repulsion between the thick zig-zag lines 1 and 2 and between the dashed lines 3 and 4 correspond to anticrossings with $\Delta I_z = 0$ and $\Delta I_z = 2$, respectively.

FIG. 2. In-phase (χ') and out-of-phase (χ'') susceptibility versus magnetic field directed along the tetragonal symmetry axis, taken at a frequency of 953 Hz and with an excitation level of 1.5 Oe. The solid lines are simulated results as described in the text.

FIG. 3. (a) Depolarization at a temperature $T = 1.8$ K and in an applied magnetic field of 20 mT. (b) Short-time depolarization for the sum of our signals at 23 mT for temperatures from 1.8 K to 20 K, highlighting the muonium oscillations. The solid lines in both (a) and (b) are the fits to the data, as described in the text.

FIG. 4. Temperature dependence of the transverse field depolarization rate versus temperature in an applied field of 23 mT. Inset: variation of the damping exponent with temperature.

FIG. 5. Field dependence of the transverse field depolarization rate versus magnetic field at a $T = 1.6$ K. Inset: variation of the damping exponent with magnetic field.

FIG. 6. Magnetic field dependence of the two observed muonium frequencies at $T = 1.8$ K.

Figure 1

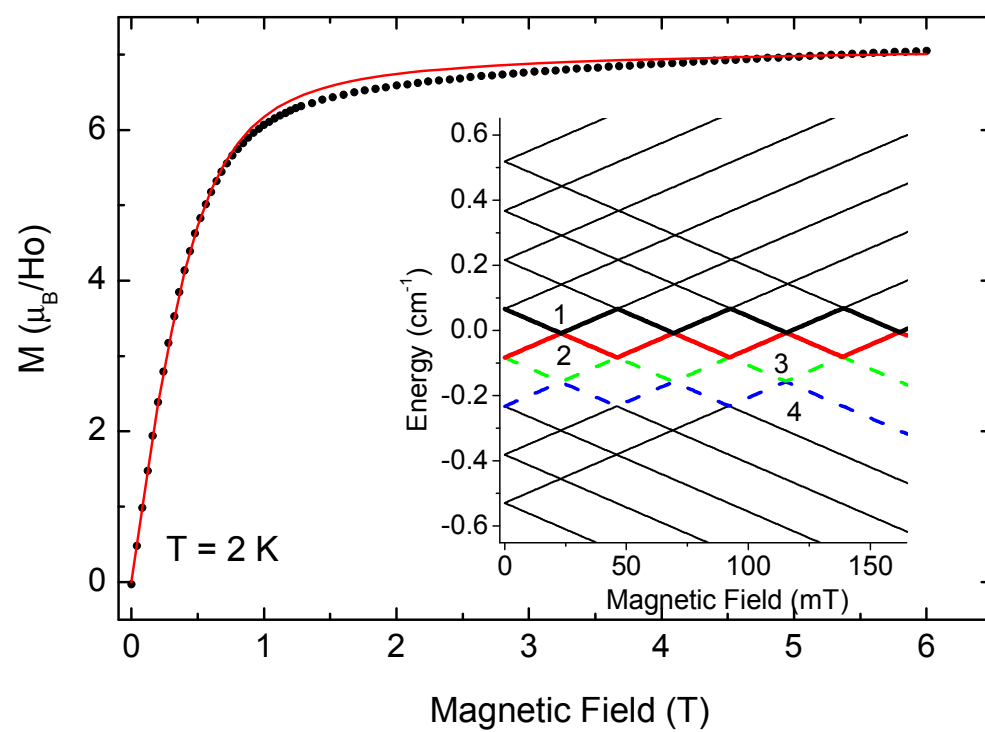


Figure 2

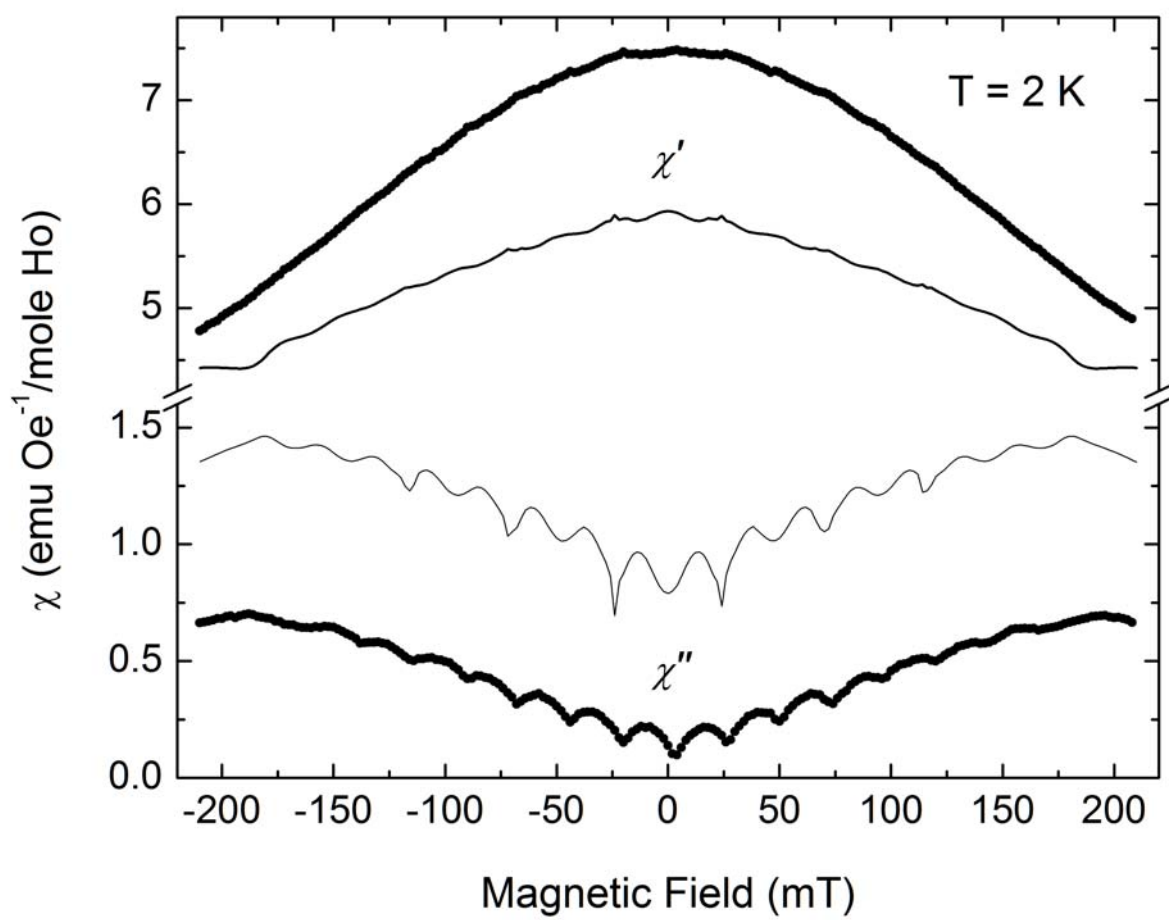


Figure 3

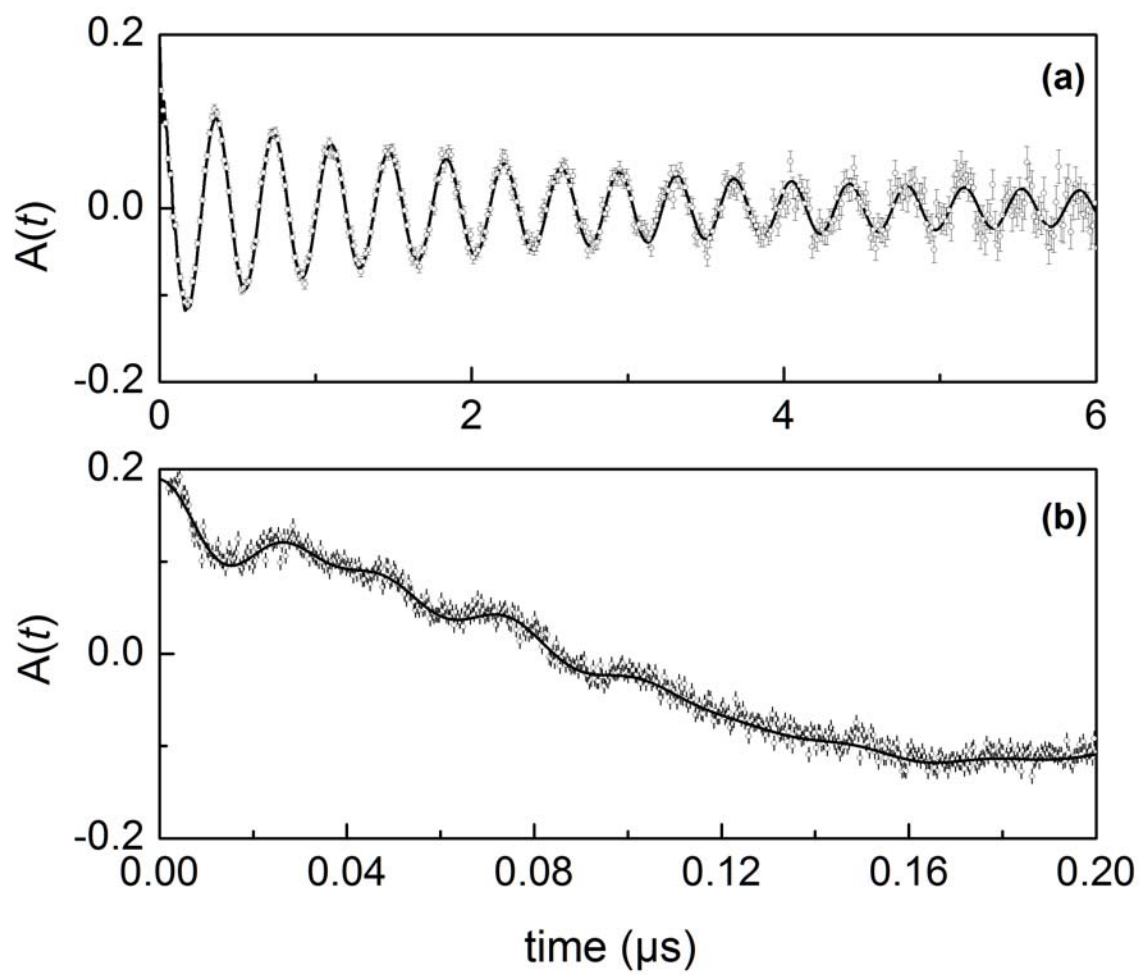


Figure 4

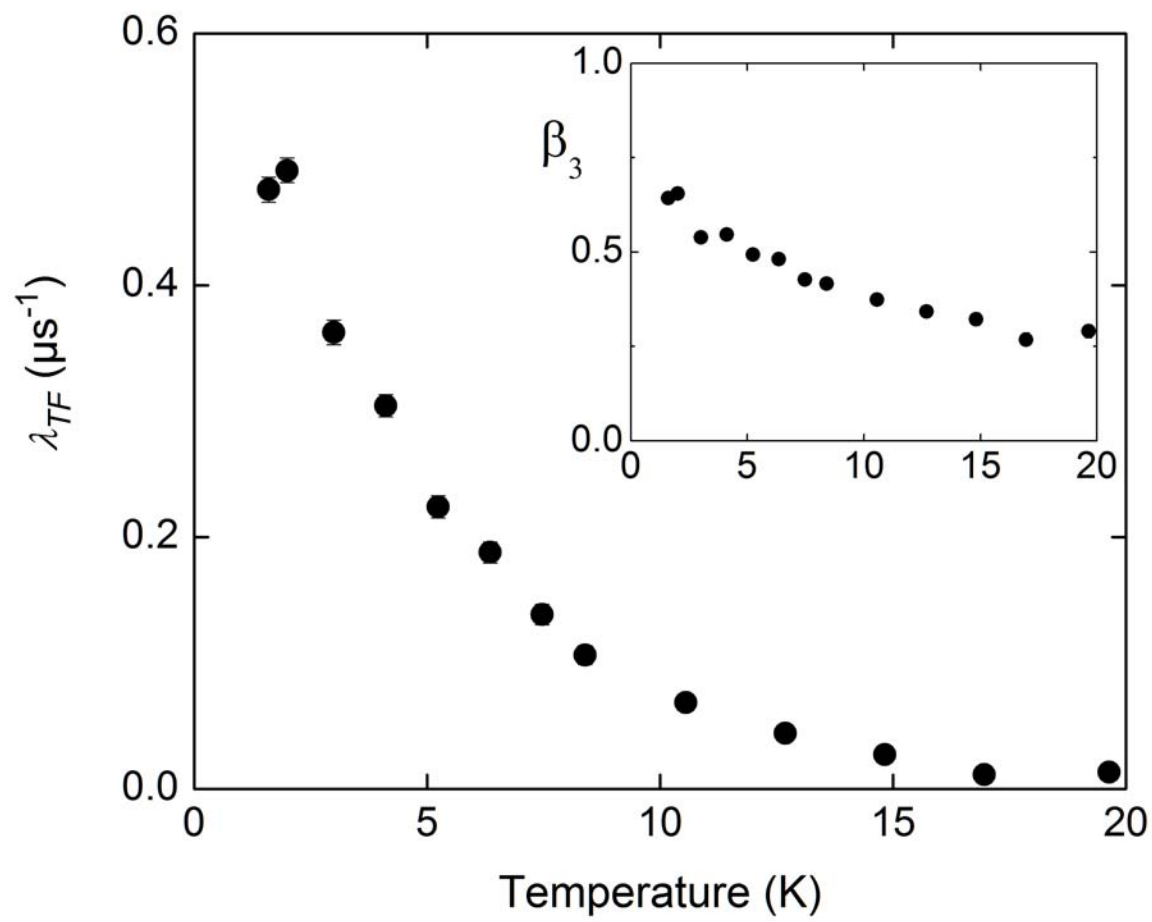


Figure 5

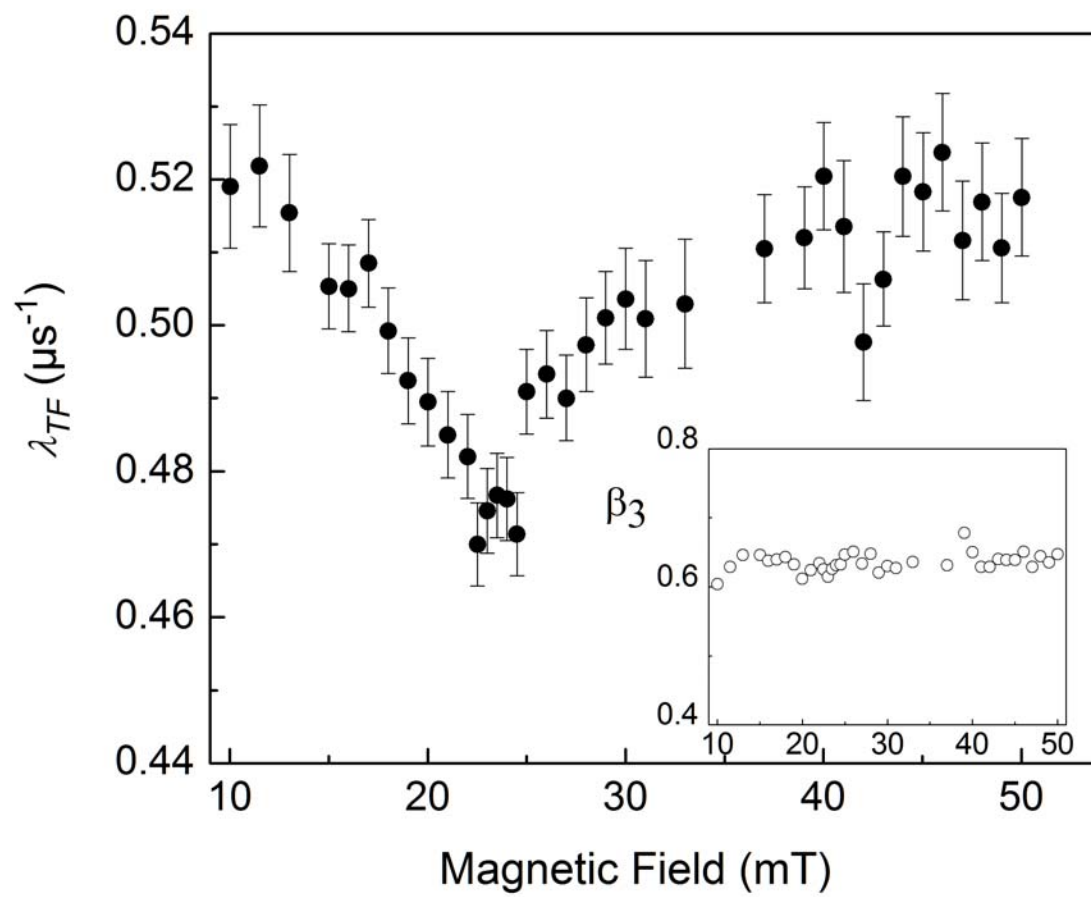


Figure 6

